Monte Carlo Study of Supramolecular Polymer Fractionation: Selective Removal of Chain Stoppers by Phase Separation

Henk J. A. Zweistra, Nicolaas A. M. Besseling,* and Martien A. Cohen Stuart

Laboratory for Physical Chemistry and Colloid Science, Wageningen University, Dreijenplein 6, 6703 HB Wagingen, The Netherlands

Received: June 28, 2006

Supramolecular polymers consist of bifunctional monomers that join and break reversibly. Supramolecular polymer solutions are often polluted by monofunctional contaminants, which drastically reduce the chain-forming capabilities of the system. Unfortunately, the monofunctional contaminants are difficult to remove due to the physical and chemical resemblance with the bifunctional counterparts. In this paper, we present a method to specifically remove the monofunctional contaminants from a supramolecular polymer solution. The general idea is to induce phase separation by decreasing the solvent quality and to remove the most dilute phase. This concept is explored by means of a recently developed Monte Carlo scheme to calculate the compositions of the coexisting liquid phases. The simulations provide a proof of principle that the proposed purification method is suitable to remove the monofunctional contaminants efficiently. The calculations indicate that, at the right experimental conditions, the vast majority of the monofunctional contaminants can be removed in this way while retaining most of the bifunctional monomers. Because of the general nature of the arguments presented here, it is to be expected that the results are applicable to a large variety of supramolecular systems. Moreover, the method is very suitable for large-scale applications because only solvent is added and no tedious chromatographic steps are required.

1. Introduction

Supramolecular polymers are linear aggregates which consist of monomers that are joined by reversible bonds. The *functionality* of a monomer is equal to the number of bonding groups of a monomer. To achieve the formation of linear chains, the monomers should be bifunctional. Many such compounds have been synthesized in recent years. Synthetic monomers usually consist of two binding groups that are connected by a spacer.[1] They can be categorized according to the nature of the reversible bond between the monomers:[1,2] hydrogen-bonded,[3−5] discotic,[6] and coordination[7] supramolecular polymers. Monofunctional monomers often occur as an unwanted by-product in the synthesis of bifunctional monomers.[1,3,8] They are detrimental to the effectivity of the supramolecular polymer system because monofunctional monomers form additional chain ends and hence reduce the average degree of polymerization. They are therefore sometimes called "chain stoppers". Controlling the amount of chain stoppers is essential to control the properties of the supramolecular polymers. It is usually very difficult to remove the monofunctional contaminants because of the large degree of chemical and physical similarity with their bifunctional counterparts.

We propose a new method to remove monofunctional contaminants from supramolecular polymer solutions. The general idea is to induce phase separation by decreasing the solvent quality and to subsequently discard the phase that is poor in polymer. The average chain length increases with concentration,[9] hence it is to be expected that the number of chain ends per monomer is larger in the dilute phase than in the concentrated phase. Because the monofunctional monomers are always at a chain end, it is to be expected that the dilute phase is enriched in monofunctional monomers. The supramolecular polymer solution can therefore be purified by inducing phase separation and to subsequently discard the dilute phase.

Phase separation methods are frequently used to purify samples of synthetic covalent polymers. In such a procedure, a large amount of poor solvent is added to a polydisperse polymer solution, which induces precipitation of the longest chains. This method is in general use to narrow down the size distribution of the polymers.[10] However, as far as we know, phase separation has not been used to specifically remove chain stoppers from supramolecular polymer solutions.

In this paper, we will explore the proposed method by simulations of a simple molecular model. The simulation results therefore do not apply to a specific system, but serve as a "proof of principle" for a broad range of experimental systems. This paper is organized as follows. In Section 2, we will first describe our simulations of phase separated supramolecular polymer solutions. From these simulations, we can construct the entire phase diagram from which the efficacy and selectivity of the method are easily determined. Unfortunately, it is not possible to simulate the purification process directly for realistic parameters of experimental systems, therefore extrapolations are necessary, as described in Section 3. These extrapolations provide a good estimate of the effectivity of the purification process in many situations.

2. Monte Carlo Simulations

2.1. Description of the Model. The idea to remove monofunctional contaminants by means of phase separation will be explored by Monte Carlo simulations. These calculations yield in principle "exact" results[11] and have been used extensively to

* Corresponding author. E-mail: klaas.besseling@wur.nl.

10.1021/jp064043z CCC: $33.50
Published on Web 08/30/2006

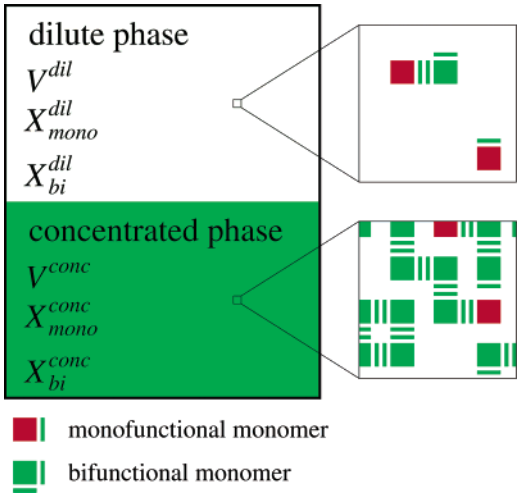

Figure 1. Schematic two-dimensional representation of the model system. An initially homogeneous supramolecular polymer solution is allowed to phase separate into a dilute and concentrated phase, each with a certain volume V and mole fractions of mono- and bifunctional monomers X_{mono} and X_{bi}.

simulate equilibrium properties of supramolecular polymers.[12−16] Moreover, in contrast with mean-field theories, the magnitude of the error does not depend on the concentration. Since the advent of the Gibbs ensemble method, simulations of coexisting liquids have been predominantly performed for continuum systems.[17] However, a lattice model is more appropriate in this case for two reasons. First, the functionality of the monomers can be implemented in a very straightforward manner in lattice systems. Second and most important, the simulation of lattice systems does not break down when one of the phases becomes very dense.[11] Until recently, simulating phase separation of lattice models proved to be quite cumbersome. Therefore, two of us developed a new method a short while ago. This method, called the "Helmholtz ensemble", enables one to simulate phase separation in lattice systems efficiently by means of Monte Carlo simulations.[18]

The supramolecular polymer solution in the presence of monofunctional monomers is modeled as follows. The solution is partitioned into cubic lattice sites. Three molecular species are present: bifunctional monomers, monofunctional monomers, and solvent molecules. Each type of molecule occupies a single site in the lattice. The molecules have six "faces" by which they make contact with their neighbors. We discriminate between several types of faces with different properties. For example, an energy penalty of $+0.5\ kT$ is assigned to each contact between a face on a monomer and a face on a solvent molecule. The solvent quality is therefore poor, and monomers and solvent molecules tend to phase separate spontaneously.

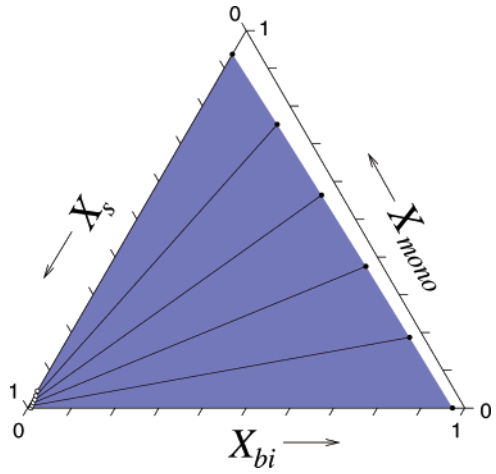

Figure 3. Phase diagram of a supramolecular polymer solution in the presence of monofunctional monomers. The bond energy is $-4\ kT$. The mole fractions of bifunctional monomers, monofunctional monomers, and solvent molecules are represented by X_{bi}, X_{mono}, and X_{s}, respectively. All possible compositions correspond to a point in this diagram. The tielines connect a composition of the dilute phase (open circles) with a composition of the coexisting concentrated phase (filled circles). The region of compositions where phase separation occurs is depicted in light blue. Any homogeneous phase with a composition inside the blue area is thermodynamically unstable and will phase separate into the dilute and concentrated phase that lie on the same tieline.

Furthermore, "linking faces" determine the connectivity of monomers. A reversible bond is formed between two adjacent monomers if linking faces on each monomer are pointed toward each other. A "bond energy" E is assigned to each reversible bond. The value of E has to be negative in order to obtain appreciable chain formation. The functionality of a monomer is in this model simply the number of linking faces that a monomer possesses: bifunctional monomers have two linking faces, while monofunctional monomers have only one (Figure 1).

2.2. Simulation Results. A simulation snapshot for $E = -6\ kT$ is shown in Figure 2. From simulations at different compositions, the entire phase diagram was calculated (Figure 3).

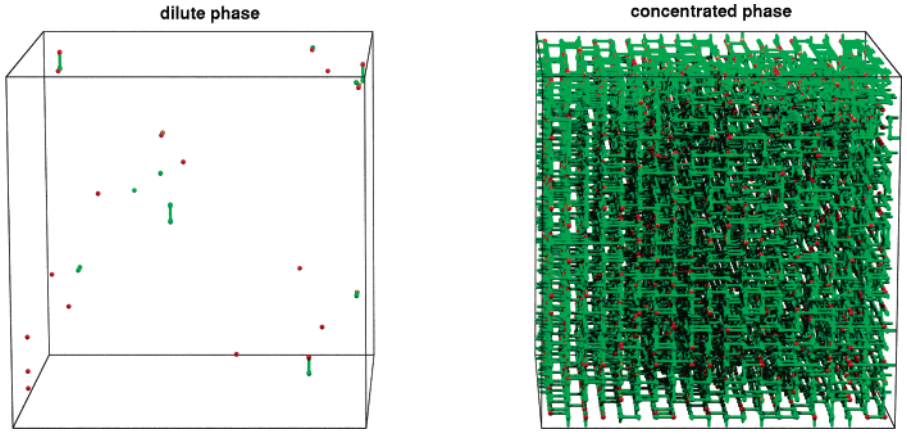

Figure 2. Snapshots of simulation boxes of the coexisting concentrated and dilute phases. Monofunctional monomers are drawn in red, bifunctional monomers in green, and the solvent is not depicted for ease of viewing. The size of the simulation boxes is $20 \times 20 \times 20$ lattice sites and the bond energy is $-6\ kT$. Note that the relative occurrence of monofunctional monomers is greater in the dilute phase than in the concentrated phase.

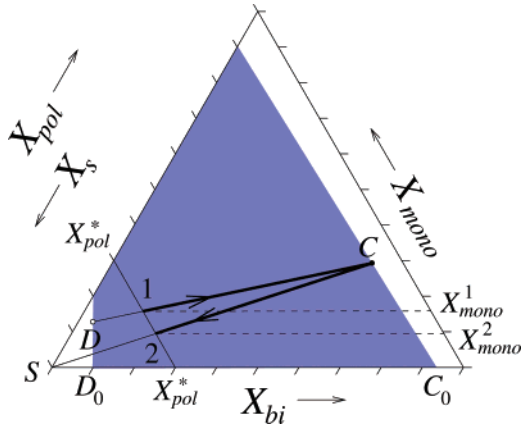

Figure 4. Cartoon of the purification method. The tieline shown in this figure is somewhat tilted for clarity. The total polymer content $X_{pol} = X_{bi} + X_{mono}$ is equal to $1 - X_s$, so the X_{pol} axis runs in the opposite direction from X_s. The purification is started in point 1 at a certain total polymer mole fraction X^*_{pol} and monofunctional monomer concentration X^1_{mono}. Point 1 lies within the phase separated region and will therefore spontaneously separate into compositions *C* and *D*. The dilute phase is removed, and the concentrated phase is diluted with solvent along the *SC* line, until the total polymer concentration is again equal to X^*_{pol} (point 2). Note that $X^2_{mono} < X^1_{mono}$ because the dilution line *SC* is steeper than the tieline *DC*.

A straight line through the lower left corner of the phase diagram can be called a "dilution line". Compositions that belong to points along such a line differ only in the concentration of solvent molecules; the ratio of mono- and bifunctional monomers remains the same. Careful inspection of Figure 3 reveals that the tielines are less steep than the dilution lines originating from any of the points on that tieline (except for the case $X_{mono} = 0$). This can be used to remove the monofunctional contaminants, as is graphically shown in Figure 4. Because the entire phase diagram is known, we can simulate an arbitrary number of purification steps according to this scheme.

The efficacy of the purification process is characterized by both the degree of purification and the yield of bifunctional monomers. Hence we define the purification parameter $p = X_{mono}/X_{bi}$ at total polymer mole fraction $X^*_{pol} = X_{mono} + X_{bi}$ (Figure 4). When the monofunctional contaminant concentration vanishes, $p \to 0$. Furthermore, the yield Y is defined as the fraction of the amount of bifunctional material that has been retained.

Figure 5 shows that p decreases with the number of purification steps n as expected. Some bifunctional monomer is inevitably discarded with the dilute phase, so the yield decreases with n as well. The volume of the dilute phase, and thus the amount of monomer that is discarded after each step, decreases with X^*_{pol}, so both p and the yield decrease faster with n when X^*_{pol} is small.

3. Analysis of the Purification Process

3.1. Parametrization of the Phase Diagram. While the results shown in Figures 3 and 5 are accurate, they underestimate the efficacy of the purification method for typical real supramolecular systems. Because of technical limitations of the Monte Carlo simulation, the bond energy in our calculations of the phase diagram was $-4\ kT$. In reality, values in the range -10 to $-20\ kT$ are found, for example, in the case of triple and quadruple hydrogen-bonding supramolecular polymers.[1,4,19,20] Because the chains are in reality longer than those in the Monte Carlo simulation, it is to be expected that the purification method will be more efficient in reality than as portrayed in Figure 5.

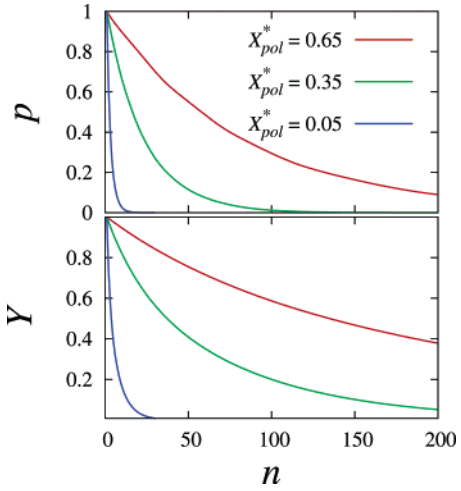

Figure 5. Plots of p and bifunctional monomer yield vs the number of purification steps. These plots were calculated directly from the phase diagram (Figure 3).

The changes of p and Y with the number of purification steps, as depicted in Figure 5, were based on extensive simulations. In the present section, it is shown that p and Y can be captured elegantly in a few simple explicit expressions. With the help of these, the number of required simulations is dramatically reduced. Moreover, systems with more negative bond energies, for which the simulations are computationally demanding, can be handled more easily.

The general idea is to characterize the phase diagram by three readily obtained parameters: C_0, D_0, and α. Parameters C_0 and D_0 are the bifunctional monomer concentrations of the coexisting phases in the absence of monofunctional contaminants (cf. Figure 4). Furthermore, α is the ratio of the slopes of the tieline (*DC*) and the dilution line (*SC*). It was checked that α is insensitive to the position in the phase diagram: for the case of $E = -4\ kT$, the deviations in α were on the order of 0.2% when moving from $X^*_{pol} = X_{mono}$ to $X^*_{pol} = X_{bi}$. Therefore C_0, D_0, and α can be regarded as intrinsic properties of the phase diagram. In the present section, we demonstrate that these parameters, together with X^*_{pol} (which one can choose), are sufficient to predict the effectivity of the purification in the limit of low chain stopper concentrations.

Let us first define $R_p = p_n/p_{n-1}$, the ratio of the p-values of two consecutive purification steps. Similarly, $R_Y = Y_n/Y_{n-1}$ is defined.

To calculate R_p, we require p_n and p_{n-1}. From Figure 4, it follows directly that $p_n = X^C_{mono}/X^C_{bi}$. On the other hand, p_{n-1}, which is equal to $X^{n-1}_{mono}/X^{n-1}_{bi}$, is calculated from the following set of equations:

$$\begin{cases} X^{n-1}_{mono} + X^{n-1}_{bi} = X^*_{pol} \\ \alpha \dfrac{X^C_{mono}}{X^C_{bi}} = \dfrac{X^C_{mono} - X^{n-1}_{mono}}{X^C_{bi} - X^{n-1}_{bi}} \end{cases}$$

After some manipulation, it is found that:

$$R_p = \frac{\alpha X^C_{mono} - X^C_{mono} + X^*_{pol}}{X^C_{bi}\left(1 - \alpha + \dfrac{\alpha X^*_{pol}}{X^C_{bi}}\right)} \qquad (1)$$

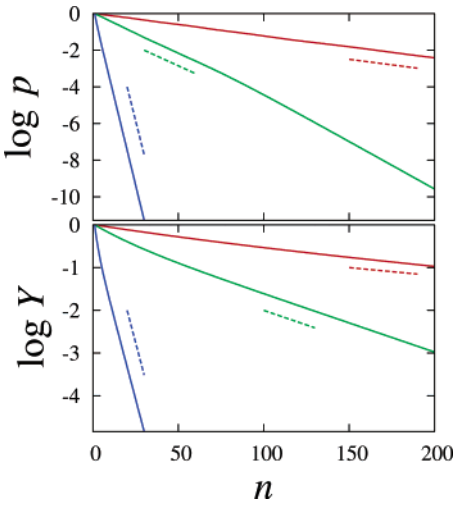

Figure 6. As in Figure 5, but here the logarithms of p and Y are plotted against n. The dashed lines denote the slope of this plot calculated by eqs 3 and 4. Equations 3 and 4 give an accurate description the purification process because the full and the dashed lines have the same slope,

The value of R_Y follows from the mass balance of the bifunctional monomers and can be shown to be:

$$R_Y = \frac{X_{bi}^{C}(X_{pol}^{*} - X_{bi}^{D})}{X_{pol}^{*}(X_{bi}^{T} - X_{bi}^{D})} \tag{2}$$

In experimental systems, the fraction of chain stoppers is usually quite low even before purification. The relevant regime is therefore $p \rightarrow 0$, hence:

$$R_p = \frac{X_{pol}^{*}}{C_0\left(1 - \alpha + \frac{\alpha X_{pol}^{*}}{C_0}\right)} \tag{3}$$

$$R_Y = \frac{C_0(X_{pol}^{*} - D_0)}{X_{pol}^{*}(C_0 - D_0)} \tag{4}$$

Figure 6 shows that decay of p and Y is exponential, hence R_p and R_Y are constants that are given by eqs 3 and 4. The decay of p and Y with n is calculated by:

$$p_n = p_0(R_p)^n \tag{5}$$

$$Y_n = (R_Y)^n \tag{6}$$

It is hereby shown that α, C_0, and D_0 (by means of eqs 3 and 4) are sufficient to describe the purification process. The parameters R_p and R_Y are central in describing the purification process because they determine the exponential decay rate of p and Y with the number of purification steps. The entire purification process can be calculated according to eqs 5 and 6. This leads to a great reduction in the computational demand of the calculation. Instead of calculating the entire phase diagram, only two simulations are needed to find C_0, D_0, and α: (i) one simulation without monofunctional monomers to find C_0 and D_0, and (ii) another simulation with monofunctional monomer to calculate α.

For a certain system at a certain temperature, the only process parameter that can be chosen is X_{pol}^{*}. Obviously, X_{pol}^{*} should be greater than D_0 but smaller than C_0. We denote the number of purification steps that are needed to achieve a reduction of the purification parameter from p_0 to p as n_{p/p_0}. The yield after n_{p/p_0} steps is then Y_{p/p_0}. For practical purposes, it is interesting to calculate the effect of our choice of X_{pol}^{*} on n_{p/p_0} and Y_{p/p_0}. Obviously, n_{p/p_0} is equal to $\log(p/p_0)/\log R_p$ (eq 5) and $Y_{p/p_0} = Y_0(R_Y)^{n_{p/p0}}$. The dependence of Y_{p/p_0} on X_{pol}^{*} is shown in Figure 7. The yield vanishes when $X_{pol}^{*} \rightarrow D_0$ since $R_Y \rightarrow 0$ in that case (eq 4). The maximum yield can be obtained when X_{pol}^{*} is chosen to be very close to the composition of the concentrated phase:

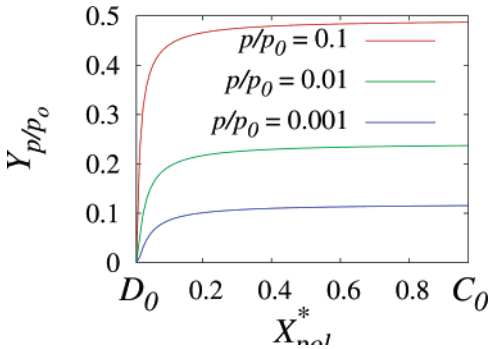

Figure 7. Plot shows the effect of the choice of X_{pol}^{*} on the yield when the purification parameter is reduced from p_0 to p. Equations 3, 4, 5, and 6 and the parameters from the phase diagram in Figure 3 were used to construct this plot. Note that the highest possible yield is obtained when $X_{pol}^{*} \rightarrow C_0$. The maximum attainable yield can be calculated directly by means of eq 7.

$$\lim_{X_{pol}^{*} \rightarrow C_0} Y_{p/p_0} = \left(\frac{p}{p_0}\right)^{D_0/(1-\alpha)(C_0-D_0)} \tag{7}$$

Therefore, the maximum yield that can be reached to reach a certain degree of purity is given by eq 7. Doing so would however require an infinite number of purification steps.

To fully exploit the possibilities of the phase diagram, we do not set X_{pol}^{*} to a fixed value for all values of E, but make X_{pol}^{*} depend on D_0 instead: $X_{pol}^{*} = \beta D_0$. We will use the parameter $\beta = X_{pol}^{*}/D_0$ to specify the choice of the polymer concentration. Obviously, $1 \leq \beta \leq C_0/D_0$. This leads to a very simple expression for R_Y in terms of β (via eq 4):

$$R_Y \approx \frac{\beta - 1}{\beta} \tag{8}$$

This is a very good approximation because $C_0 \approx 1 \gg D_0$, therefore, the approximation sign in eq 8 can be considered an equal sign for all practical purposes. Hence R_Y is found without any extrapolations necessary.

3.2. Predictions for Realistic Systems. It was shown that the phase diagram can be described by the three parameters C_0, D_0, and α for calculating the effectivity of purification. It is in principle possible to extrapolate all three parameters to realistic bond energies and then calculate R_p and R_Y. However, estimating R_p and R_Y in this way is dangerous because it depends on three different extrapolations. It is therefore preferable to extrapolate R_p directly and calculate R_Y according to eq 8, for which no extrapolations are necessary.

To estimate R_p, we first calculated C_0, D_0, and α for a range of bond energies. The simulations were performed as described in Section 2, but with larger simulation boxes of $25 \times 25 \times 25$ lattice sites. We then calculated R_p by means of eq 3 and plotted R_p versus E (Figure 8). The calculated values for R_p for different

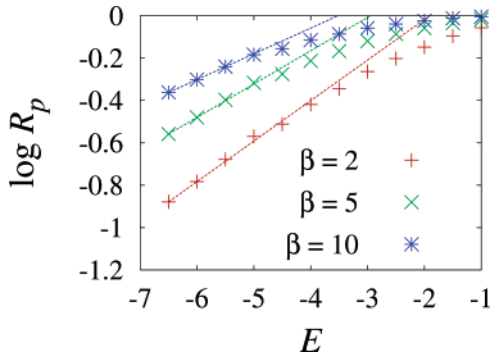

Figure 8. Values of R_p (calculated with eq 3) are plotted logarithmically vs bond energy. Fits of R_p with emphasis on the low E regime are taken from Table 1 and shown by dashed lines. See text for computational details.

TABLE 1: Coefficients *a* and *b* from Eq 9 for Different β

β	a	b
2	2.316	0.1913
5	2.911	0.1573
10	2.677	0.1215

E were empirically fitted to the expression

$$R_p = a10^{bE} \tag{9}$$

Coefficients a and b are shown in Table 1.

Because R_p and R_Y are now known, we can estimate the purification process at realistic bond energies. Figure 9 shows the dependence of n and Y on p/p_0 for $E = -20\ kT$. It can be inferred from Figure 9 that we can expect to remove 99.9% of the chain stoppers ($p/p_0 = 10^{-3}$) and retain more than 50% of the bifunctional monomers after only one purification step if $\beta = 2$. If β is higher, that is, if less solvent is added in a single purification step, then a higher yield is possible. This would require only a few purification steps to reach the same level of purification.

It is clear that the volume of the concentrated phase will be much smaller than the volume of the dilute phase, even if $\beta = 10$. We recommend therefore that experimental conditions must be chosen so that the volume of the dilute phase is much greater than the volume of the concentrated phase. Which conditions should be chosen depends on the system and on the technical demands of the process. Once a suitable value of β is determined, one should determine D_0 by determining the concentration of supramolecular monomers in the dilute phase. With $X^*_{\mathrm{pol}} = \beta D$ now known, there is enough information to set up the extraction process for this specific system.

4. Summary and Outlook

In the previous sections, we have put forward a new method to remove monofunctional contaminants from supramolecular polymer solutions. The method exploits the partitioning of mono- and bifunctional monomers over the two phases of a phase-separated supramolecular polymer system. The polymer solution can be purified by discarding the dilute phase because that phase is enriched in monofunctional contaminants.

By means of a recently developed numerical technique, we calculated the entire phase diagram of a ternary mixture containing mono- and bifunctional monomers and solvent. The purification process can be simulated directly from the phase diagram (Section 2).

Moreover, we were able to describe the purification process in terms of simple mathematical expressions with only three parameters. Only two simulations are necessary to find these parameters (Section 3.1). The effectivity of purification could therefore be calculated and extrapolated for a broad range of bond energies.

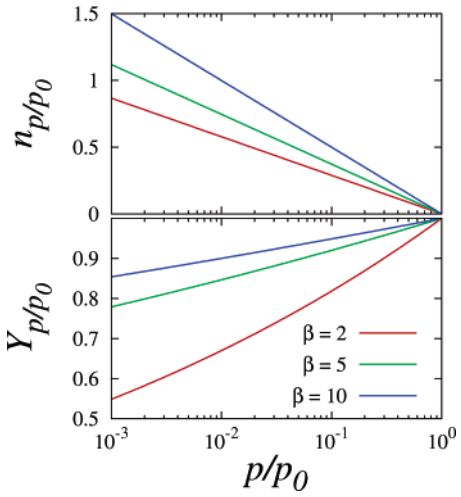

Figure 9. Predicted purification efficacy for $E = -20\ kT$. The value n_{p/p_0} is the number of purification steps that is needed to achieve a reduction of the purification parameter from p_0 to p. The yield after n_{p/p_0} steps is Y_{p/p_0}.

Our calculations indicate that one or two purification steps are sufficient to remove 99% of the chain stoppers while retaining about 80% of the bifunctional monomers in many experimental systems (Section 3.2). Higher yields are definitely possible if less solvent is added. However, some more purification steps are then required to reach the same purity of the sample.

The extraction method only involves the addition of solvent, so it is cheap to perform and could be easily scaled up to industrial quantities. It also does not require the addition of other chemicals that have to be removed afterward. In conclusion, the calculations presented in this paper show that the present method is most likely a viable methodology to selectively and efficiently remove monofunctional ligands from supramolecular polymer solutions.

The next challenges are both computational and experimental. It would be of interest to assess the effect of solvency (which is not addressed in this paper) and/or more complex molecular models on the effectivity and selectivity of purification. Finally, it is imperative to apply and test this method in experimental systems.

References and Notes

(1) Brunsveld, L.; Folmer, B. J. B.; Meijer, E. W.; Sijbesma, R. P. *Chem. Rev.* **2001**, *101*, 4071−4097.

(2) Ciferri, A. Mechanisms of Supramolecular Polymerizations. In *Supramolecular Polymers*; Ciferri, A., Ed.; Marcel Dekker: New York, 2000; Chapter 1.

(3) Sijbesma, R.; Beijer, F. H.; Brunsveld, L.; Folmer, B. J. B.; Ky Hirschberg, J. H. K.; Lange, R. F. M.; Lowe, J. K. L.; Meijer, E. W. *Science* **1997**, *278*, 1601−1604.

(4) Corbin, P. S.; Zimmerman, S. C. Hydrogen-Bonded Supramolecular Polymers. In *Supramolecular Polymers*; Ciferri, A., Ed.; Marcel Dekker: New York, 2000; Chapter 4.

(5) Fogleman, E. A.; Yount, W. C.; Xu, Y.; Craig, S. L. *Angew. Chem., Int. Ed.* **2002**, *41*, 4026−4028.

(6) van de Craats, A.; Warman, J. C.; Fechtenkötter, A.; Brand, J. D.; Harbison, M. A.; Müllen, K. *Adv. Mater.* **1999**, *11*, 1469−1471.

(7) Vermonden, T.; van der Gucht, J.; de Waard, P.; Marcelis, A. T. M.; Besseling, N. A. M.; Sudhölter, E. J. R.; Fleer, G. J.; Cohen Stuart, M. A. *Macromolecules* **2003**, *36*, 7035.

(8) Armstrong, G.; Buggy, M. *J. Mater. Sci.* **2005**, *40*, 547−559.

(9) Cates, M. E.; Candau, S. J. *J. Phys.: Condens. Matter* **1990**, *2*, 6869−6892.
(10) des Cloizeaux, J.; Jannink, G. *Polymers in Solution;* Clarendon Press: Oxford, 1990.
(11) Frenkel, D.; Smit, B. *Understanding Molecular Simulation*; Academic Press: London, 2002.
(12) Milchev, A.; Landau, D. P. *J. Chem. Phys.* **1996**, *104*, 9161−9168.
(13) Rouault, Y.; Milchev, A. *Macromol. Theory Simul.* **1997**, *6*, 1177−1190.
(14) Wittmer, J. P.; Milchev, A.; Cates, M. E. *J. Chem. Phys.* **1998**, *109*, 834−845.
(15) Milchev, A.; Wittmer, J. P.; van der Schoot, P.; Landau, D. P. *Europhys. Lett.* **2001**, *54*, 58−64.
(16) Lü, X.; Kindt, J. T. *J. Chem. Phys.* **2004**, *120*, 10328−10338.
(17) Panagiotopoulos, A. Z. *Mol. Phys.* **1987**, *61*, 813−826.
(18) Zweistra, H. J. A.; Besseling, N. A. M. *Phys. Rev. E* **2006**, *74*, 016111.
(19) Jorgensen, W. L.; Pranata, J. *J. Am. Chem. Soc.* **1990**, *112*, 2008−2010.
(20) Pranata, J.; Wierschke, S. G.; Jorgensen, W. L. *J. Am. Chem. Soc.* **1991**, *113*, 2810−2819.